Interaction of Lanthanum with Boron and Carbon: Phase Diagram and Structural Chemistry

Volodymyr Babizhetskyy, Arndt Simon, Josef Bauer

Interaction of Lanthanum with Boron and Carbon: Phase Diagram and Structural Chemistry

Volodymyr Babizhetskyy ● Arndt Simon ● Josef Bauer

Received: ……/Accepted …

Abstract

The isothermal section of the La–B–C phase diagram at 1270 K has been investigated by means of X-ray, neutron powder diffraction, microstructure and EPMA analyses. Eight ternary compounds were found, and for six of them the crystal structures have been established. The phase with the structure type of $La_5B_2C_6$ has a broad homogeneity range described by the formula $La_5(BC)_x$ ($5.6 \leq x \leq 8.8$). The lanthanum sesquicarbide La_2C_3 exhibits an extended solid solution in the ternary domain $La_2C_{3-x}B_x$ ($x=0.4$). The boron substitution of carbon leads to the decrease of the superconducting temperature from 13.4 K for La_2C_3 to 10.0 K for $La_2C_{2.8}B_{0.2}$ and from 5.6K for $La_2C_{2.7}$ to 4.1K for $La_2C_{2.6}B_{0.4}$. The compositions of two new compounds, ~$La_4B_3C_{12}$ and ~$La_4B_5C_{18}$ were found via WDX analysis.

Keywords: Carbides ● Solid state ● Crystal structure ● Phase diagrams

V. Babizhetskyy (✉)
Department of Inorganic Chemistry, Ivan Franko National University of Lviv, Kyryla & Mefodiya Str. 6, UA-79005 Lviv, Ukraine
E-mail address: v.babizhetskyy@googlemail.com
V. Babizhetskyy, A. Simon
Max-Planck-Institut für Festkörperforschung, Heisenbergstrasse 1, Postfach 800665, D-70569 Stuttgart, Germany
J. Bauer
Laboratoire de Chimie du Solide et Inorganique Moléculaire, UMR CNRS 6511, Université de Rennes 1-ENSCR, Institut de Chimie, Campus de Beaulieu, Avenue du Général Leclerc, F-35042 Rennes Cedex, France

Introduction

The search for new ternary boride carbides predicted from several structural models recently led to a systematic study of ternary phase diagrams, especially of carbides, borides and boride carbides. The structures of the ternary rare earth (*RE*) boride carbides display a variety of different arrangements with boron carbon substructures. They extend from zero-dimensional units to chains and two-dimensional nets embedded in the metal atom sublattices as well as interconnected boron icosahedra [1, 2]. The substructures can be divided into three groups. In the first group the finite (0-D) quasi-molecular entities fill voids of the metal atom matrix and can have different lengths ranging from 2 to 13 non-metal atoms. Stretched units of different sizes as well as isolated C atoms can coexist. In the second category, the non-metal atoms form infinite one-dimensional planar or nearly planar ribbons $(BC)_\infty$ of zigzag chains of boron atoms to which carbon atoms are attached. In the third family, the boron and carbon atoms form infinite planar (2-D) nets which alternate with sheets of metal atoms.

The phase relations in the general *Ln*-B-C systems were not studied in sufficient detail so far. The solid-state phase equilibria in the ternary phase diagrams with *Ln* = Y, Eu, Gd, Ho were reported [3 - 6]. The crystal structures of the known La-containing compounds were determined from X-ray single crystal data. Two essential structural features of the model for LaB_2C_2 solved in space group $P\bar{4}2c$ presented in [7] remain uncertain. They adress the questions, firstly, whether B and C atoms within the eight-membered rings are alternating or arranged in pairs and, secondly, whether B and C atoms are stacked identically or alternatingly along *c*. The reexamination of the LaB_2C_2 structure using neutron powder diffraction has been performed [8]. The underlying coloring problem in extended networks and the correlation between symmetry and electronic stability has been thoroughly treated by Burdett et al. [9], and on the basis of Extended Hückel calculations they reached the conclusion that a coloring scheme with only heteroatomic B-C bonds in contrast to [7] should represent the stable pattern in the LaB_2C_2 structure family. Refinements in *P*4/*mbm* are in agreement with the predicted structure

characterized by only heteroatomic B-C bonds, however, in distorted 2-D squares and octagons, in contrast to the structural model proposed in [8].

From the first category with 0-D quasi-molecular entities, the phase $La_5B_2C_6$ containing CB_3 units and isolated carbon atoms has recently been described in detail [10, 11]. The atom displacements in the structure are indeed due to real structure effects and are not a consequence of experimental artefacts (e. g. absorption) or inappropriate structure models (e. g. wrong choice of space group, superstructures, or twinning). Tetragonal rare earth boride carbides with structure types derived from ~$La_5B_2C_6$ and Sc_3C_4, respectively, can intergrow coherently. Slabs of both types with various thicknesses from one unit cell up to macroscopic domains may occur, sharing a common square net of metal atoms [12]. In the crystal structures additional $La_xB_yC_z$ compounds were found with B/C chains of different lengths. So, the structure of LaBC contains non-linear B_5C_5 chains [13]. The structure of $La_{10}B_9C_{12}$ contains slightly corrugated two-dimensional metal atom square nets forming two types of chains with 26 and 18 La atoms, respectively, wherein B_4C_4 and B_5C_8 units are located [14]. The structure of $La_5B_4C_{5-x}$ (x = 0.15) is composed of slightly corrugated two-dimensional metal atom square nets hosting the finite boron-carbon units B_4C_4, B_3C_3, BC_2 and isolated carbon atoms. The positions of the carbon atoms in the unit BC_2 are not fully occupied [15]. Longer oligomeric anions are observed when the boron-carbon ratio increases. Eleven-membered chains of different B/C ratio, B_4C_7 and B_5C_6, exist in $La_{15}B_{14}C_{19}$ [16].

In order to pursue our systematic research on the $La_xB_yC_z$ phases, we focused on the solid-state phase equilibria in the ternary La-B-C phase diagram. Hence, the presentation of the isothermal section of the ternary La-B-C phase diagram at 1270 K, crystallographic data of the ternary compounds and the structure and determination of the homogeneity range of ~$La_5B_2C_6$ are subjects of this work.

Results and discussion

Phase equilibria in the the La-B-C ternary system

The isothermal section of the La-B-C phase diagram at 1270K is presented in Fig. 1. In agreement with Schlesinger et al. [17], two binary compounds, LaB_4 and LaB_6 have been found in the La–B binary system at 1270K. The existence of two binary compounds, La_2C_3 and LaC_2, have been confirmed according to the data of Gschneidner et al. [18]. The superconducting properties of the rare earth sesquicarbide and homogeneity region of $La_2C_{3-\delta}$ (T_c=13.4 K for La_2C_3 and 5.6K for $La_2C_{2.7}$) were recently studied [19, 20]. The standardized cell parameters at 293K (Germanium 99.9999%, a_{Ge}=5.657905 Å, served as internal standard) for $La_2C_{3-\delta}$ changes from a=8.8149(5) for La_2C_3 to 8.8079(5)Å for $La_2C_{2.7}$. The results of EPMA analysis show that this phase is extended in a ternary domain. The influence of the boron addition at the $La_2C_{3-\delta}$ was also observed by magnetic measurements of crushed alloys buttons. So, the boron substitution in La_2C_3 leads to the composition $La_2C_{2.8(1)}B_{0.2(1)}$ (a=8.8136(4) Å) and decreasing T_c from 13.4 K to 10.0 K. For $La_2C_{2.7}$ a limit of the homogeneity was observed at $La_2C_{2.6}B_{0.4(1)}$ (a=8.8218(6) Å), the phase becoming superconducting at 4.1 K in contrast to T_c = 5.6 of $La_2C_{2.7}$ [19]. The results will be published separately. A very small range of homogeneity of LaC_2 was detected by neutron and physical properties experiments [21]. No extension of a ternary domain has been detected for the binary compound ″B_4C″ [22, 23]. The phase boundary of the La-rich liquid was not defined within the ternary system. The micrograph analysis was unsuccessful because of high sensitivity of samples against moisture. The form of the solid phases arrangements below 1190 K is sketched in Fig. 1 by dashed lines corresponding to the literature data of binary systems presented in [17, 18].

< Fig. 1 >

Metallographic investigation, X-ray powder diffraction and EPMA analyses revealed the new compound ~$La_7B_9C_{34}$ to be in equilibrium with LaB_6 (Fig.2 a, b). Fig. 2 c, d shows the three-phase region of the La-B-C ternary system between LaB_4, LaBC and La confirmed by X-ray powder diffraction and EPMA analyses.

The crystallographic characteristics of the ternaries in the La-B-C system are listed in Table 1. It is worth noting that after annealing at 1270 K the phase $La_{15}B_{14}C_{19}$ [16] was not found. It exists only in arc-cast samples. The compositions of two new compounds ~$La_4B_3C_{12}$

< Fig. 2 >

and ~$La_4B_5C_{18}$ were found using WDX analysis. They show up in the phase diagram according to Fig. 1.

Solid solution $La_5(BC)_x$ ($5.6 \leq x \leq 8.8$)

$RE_5B_2C_6$ was first discovered and labeled as "Gd_2BC_2" [5a]. The phase exhibits a large homogeneity region. The X-ray powder diagrams of "RE_2BC_2" show a similarity with

< Table 1 >

corresponding rare earth dicarbides (CaC_2 type structure) with an observed *a* parameter slightly smaller than in REC_2 and doubled *c* parameter. Firstly, the crystal structure of ~$La_5B_2C_6$ has been determined in space group *P*4 from single crystal x-ray data [24] and the correct formula and superconducting transition at 6.9 K was deduced. Later, the structure of ~$La_5B_2C_6$ [10] was reinvestigated in space group *P*4/*ncc* (*a* = 8.590, *c* = 12.398 Å). Crystal structure and real structure investigations on the intermittent superconductivity of ~$La_5B_2C_6$ indicated in [11]

clearly show that superconductivity is not an intrinsic property of the phase, but must be ascribed to precipitations of a B containing La_2C_{3-x} phase in the C rich region and β-La in the metal-rich region. Obviously, the complete coverage of borocarbide crystallites by La can result in a total magnetic shielding of the samples

< Fig. 3 >

The structural arrangement of ~$La_5B_2C_6$ compounds consists of a three-dimensional framework of rare-earth atoms resulting from the stacking of slightly corrugated two-dimensional squares, which lead to the formation of octahedral voids and distorted bicapped square antiprismatic cavities (Fig. 3 a-c). They are filled with isolated carbon atoms and twofold disordered CBCC units, respectively. The C1, C2/B2 atoms in ~$La_5B_2C_6$ form bent CBCC units with C/B-C distances of 1.32 Å indicative of double bond character and C/B - C/B distances of 1.65 Å. The C– C/B – C/B angle is 158.1°.

Unambiguous locations of C/B in Wyckoff position 16*g* in disordered CBCC units as well as occupation of light atoms are not always obvious from the X-ray measurements. Therefore supplementary powder neutron and synchrotron single crystal experiments were performed. The

< Table 2 >

< Table 3 >

results of the structure refinement are in good agreement with WDX analyses. Tables 2 and 3 present the results of Rietveld refinements of x-ray, neutron and synchrotron single crystal

investigations of ~$La_5B_2C_6$. The unit cell parameter *c* for ~$La_5B_2C_6$ varies significantly and ranges from 12.315(2) to 12.843(4) Å. However, the occupation of the large voids by only disordered CBCC units is improbable. The observation of large displacement parameters for the central C/B atoms of the CBCC units is in line with the disorder of occupation by either CBC or CBCC units for the large voids and single carbon atoms in octahedral voids. That is the reason for the large homogeneity region of this compound. The structure refinement clearly shows that for the unit cells with $c/a<1.474$ the BC_3 unit does not fully occupy the La_{10} voids (Fig. 3c). The boron content in $[C=B–C=C]^{7-}$ varies from 15(1) to 21(1) at % which leads to a decrease in charge as well as disorder [5]. The overall charge of the anionic part seems to be compensated by introduction of single carbon atoms (C3) in La octahedra. The octahedron volume increases from 30.524Å^3 for empty octahedra to 32.146Å^3 for fully occupied ones by C3 atoms (Fig. 3b). So, the homogeneity region of ~$La_5B_2C_6$ is defined as $La_5(BC)_x$ ($5.6\leq x\leq 8.8$) and presented in Fig. 1.

Conclusion

The isothermal section of the La–B–C phase diagram at 1270 K has been investigated by means of X-ray, neutron powder diffraction, microstructure and EPMA analyses. In the system eight ternary compounds were found. For six of them, namely ~$La_5B_2C_6$, $La_5B_4C_5$, LaBC, $La_{10}B_9C_{12}$, $La_{15}B_4C_{14}$, LaB_2C_2, the crystal structures have been established. The phase $La_5B_2C_6$ has a wide homogeneity range described by the formula $La_5(BC)_x$ ($5.6\leq x\leq 8.8$). For the boundary compounds of the La-B system no extension in the ternary domain was found. In contrast to binary borides the lanthanum sesquicarbide La_2C_3 exists as solid solution $La_2C_{3-x}B_x$ (x=0.4). The carbon substitution by boron leads to a decrease in T_c from 13.4 K for La_2C_3 to 10.0 K for $La_2C_{2.8}B_{0.2}$ and from 5.6K for $La_2C_{2.7}$ to 4.1K for $La_2C_{2.6}B_{0.4}$. The new compounds ~$La_4B_3C_{12}$ and ~$La_4B_5C_{18}$ show broad diffraction peaks. In contrast to the rare earths with small atomic radius lanthanum boride carbides form no compounds with infinite one-dimensional planar or nearly planar ribbons $(BC)_\infty$. The investigated structures contain finite (0-D) quasi-molecular B/C entities which fill voids of the lanthanum matrix and can have different lengths ranging from

2 to 13 non-metal atoms. Linear or bent units of different sizes as well as isolated C atoms can coexist.

Experimental

Synthesis and analysis

Polycrystalline samples were prepared from commercially available pure elements: lanthanum with a claimed purity of 99.99 at%, Alfa – Aesar, Johnson Matthey Company, sublimed bulk pieces; crystalline boron powder, purity 99.99 at%, H. C. Starck, Germany; graphite powder, purity 99.98 at%, Aldrich. Before use, the graphite and boron powders were outgased overnight at 1220 K, $p < 10^{-5}$ mbar. Lanthanum ingots were filed to coarse powders with beryllium bronze files (Dönges GmbH, Germany). Stoichiometric mixtures of the constituents were compacted in stainless steel dies. The pellets were arc-melted under purified argon atmosphere [25] on a water-cooled copper hearth. The alloy buttons of 1g were turned over and remelted three times to improve homogeneity. The samples were then wrapped in molybdenum foil and annealed in silica tubes under argon for 1 month at 1270 K. Subsequent heating for some samples just above the melting point was carried out in a high-frequency furnace (TIG-10/300, Hüttinger, FRG) under argon atmosphere for several hours at different temperatures. Finally, the samples were wrapped in molybdenum foils, annealed in evacuated silica tubes for one month at 1270 K and subsequently quenched in cold water. Sample handling was carried out under argon atmosphere in a glove box (P_{H2O}<0.1 ppm) or through the Schlenk technique.

X-ray powder diffraction patterns were obtained on a powder diffractometer STOE STADI P with Mo$K_{\alpha 1}$ radiation, using capillaries sealed under dried argon to avoid hydrolysis. The unit cell parameters for the investigated compounds $La_xB_yC_z$, as well as the Rietveld refinements for some samples containing the $La_5B_2C_6$ phase were refined with the help of the CSD program package or FULLPROF programs packages [26, 27]. The results are given in Tables 1, 2.

< Fig. 4 >

For neutron powder experiments the ^{11}B containing sample ~$La_5B_2C_6$ of 10 g was sealed into a vanadium can under 1 bar of He and measured at 300 K using the GEM diffractometer at the ISIS laboratory. The structural parameters as well as the composition were gained from Rietveld refinements using the FULLPROF program. Figure 4 shows the neutron powder diffraction patterns of composition $La_5B_2C_{6-x}$. The refined parameters of the $La_5B_2C_{6-x}$ (x = 1.4) phase include the lattice constants, the fractional coordinates of the La, B/C and C atoms, isotropic displacement parameters, (anisotropic in case of La). After refinements with the aforementioned parameters, in a last step, the C occupancy was refined and the convergence by varying the occupancy was checked in those cases where the other refined parameters are fixed or free. For both cases, a C deficiency in 4*c* and 16*g* sites is derived consistently. The results of the refinements at *T*=300 K are listed in Table 1. The single crystal diffraction data of $La_5B_{2-x}C_{6-y}$ were collected at room temperature on a synchrotron facility with λ = 0.41328Å. The starting atomic parameters taken from [10] were refined with the program SHELX-97 [28] within the WinGX program package [29] (full matrix least-squares on F^2) with anisotropic atomic displacements for La atoms. The atomic coordinates and atoms displacement parameters are listed in Tables 3 and 4.

Microprobe analysis.

For metallographic inspection and electron probe microanalysis (EPMA) some alloys were embedded in Woods metal (Fluka Chemie, Switzerland) with a melting point of ca. 75°C. The samples were polished on a nylon cloth using chromium oxide (Bühler Isomet) with grain sizes 1-5 μm. Quantitative and qualitative composition analyses of the samples were performed by energy dispersive X-ray spectroscopy (EDX) and wavelength dispersive X-ray spectroscopy

(WDX) on a scanning electron microscope TESCAN 5130 MM with an Oxford Si-detector and with an Oxford INCA WAVE 700 detector. LaB_4 and LaB_2C_2 standards were used to deduce the compositions of compounds. For the chemical microprobe, the polishing procedure had to be performed or repeated just before the measurements. Metallographic and EPMA analyses of the La-B-C ternary system reveal the compound LaBC [13] to be in phase equilibrium with $La_5B_4C_5$ [15], $La_{10}B_9C_{12}$ [14] and $La_5(BC)_x$ ($5.6 \leq x \leq 8.8$) ($La_5B_2C_6$ structure type) [11] and LaB_4 at 1270K. Metallographic and EPMA analyses are in good agreement with results from x-ray powder diffraction (*e. g.* see Fig. 2). Chemical analysis of the sample $La_5B_{2.4}C_{5.3}$ ($La_5B_2C_6$ structure) was performed in the Mikroanalytisches Labor Pascher in Remagen-Bandorf, Germany. The results of the EPMA and chemical analyses are listed in Tabl. 2.

Magnetical properties.

The magnetic properties were studied in the temperature interval 1.8 - 330 K by use of a MPMS XL-7 SQUID magnetometer (Quantum Design, Inc.) in external fields up to 7 T. The crushed alloys buttons of irregular shapes were used for the measurements.

Acknowledgements

The authors gratefully thank M. Babizhetska for the sample preparation, Dr. C. Hoch for X-ray intensity data collection, E. Brücher for the magnetization measurements, V. Duppel for EPMA analysis.

References

[1] Bauer J, Halet J-F, Saillard J-Y (1998) Coord Chem Rev 178–180:723

[2] Mori T, (2008) Higher borides. In: Gschneidner K A Jr, Bunzli J-C, Pecharsky V (eds) Handbook on the Physics and Chemistry of Rare Earths. North-Holland, Amsterdam, p. 105

[3] Bauer J, Nowotny H (1971) Monatsh Chem 102: 1129

[4] Schwetz K A, Hoerle M, Bauer J (1979) Ceramurgia Intl 5 (3):105

[5] a) Smith P K, Gilles P W (1967) J Inorg Nucl Chem 29:375

b) Ruiz D, Garland M. T, Saillard J-Y, Halet J.-F, Bohn M, Bauer J (2002) Solid State Sciences 4:1173

[6] Bauer J, Vernnegues P, Vergneau J. L (1985) J Less Comm Met 110:295

[7] Bauer J, Bars O (1980) Acta Crystallogr Sec B 36:1540

[8] Onoyama K, Kaneko K, Indoh K, Yamauchi H, Tobo A, Onodera H, Yamaguchi Y (2001) J Phys Soc Japan 70:3291

[9] Burdett J K, Canadell E, Hughbanks T (1986) J Am Chem Soc 108:3971

[10] Oeckler O, Bauer J, Mattausch Hj, Simon A (2001) Z Anorg Allg Chem 627:779

[11] Simon A, Babizhetskyy V, Oeckler O, Mattausch Hj, Bauer J, Kremer R K (2005) Z Anorg Allg Chem 631:316

[12] Oeckler O, Duppel V, Bauer J, Mattausch Hj, Simon A (2002) Z Anorg Allg Chem 628:1607

[13] Babizhetskyy V, Mattausch Hj, Gautier R, Bauer J, Halet J-F, Simon A (2005) Z Anorg Allg Chem 631:1041

[14] Babizhetskyy V, Mattausch Hj, Simon A (2004) Z Kristallogr NCS 219:11

[15] Babizhetskyy V, Mattausch Hj, Simon A (2003) Z. Kristallogr NCS 218:417

[16] Gougeon P, Halet J-F, Ansel D, Bauer J Z. Kristallogr (1996) NCS 211:822

[17] Schlesinger M E, Liao P K, Spear K E (1999) Journal of Phase Equilibria 20:73

[18] Gschneidner K A Jr, Calderwood F W (1986) Bull All Phase Diagr 7:446

[19] Simon A, Gulden Th (2004) Z Anorg Allg Chem 630:2191

[20] Kim J S, Xie W-H, Kremer R K, Babizhetskyy V, Jepsen O, Simon A, Ahn K S, Raquet B, Rakoto H, Broto J M, Ouladdiaf B (2007) Phys Rev B 76(1):014516/1

[21] Babizhetskyy V, Jepsen O, Kremer R K, Simon A, Ouladiaff B, Stolovits A (2014) J Phys Condens Matter 26:025701

[22] Morosin B, Kwei G H, Lawson A C, Aselage T L, Emin D (1995) J Alloys Compd 226:121

[23] Sologub O, Michiue Y, Mori T (2012) Acta Cryst E68:i67 and references therein

[24] Bauer J, Bars O (1983) J Less-Common Met 95:267

[25] Horvath B, Strutz J, Geyer-Lippmann J, Horvath G (1981) Z Anorg Allg Chem 483:205

[26] Akselrud L G, Grin Yu N, Zavalii P Yu, Pecharskii V K (1993) WinCSD – Universal Program Package for Single Crystal and/or Powder Structure Data Treatment, Materials Science Forum 335:133

[27] Rodriguez-Carvajal J (1993) Phys B 192:55

[28] Sheldrick G M (1997) SHELXL-97, Program for the Refinement of Crystal Structures, University of Göttingen (Germany)

[29] Farrugia L J (1999) WinGX (Version 1.64.05), J Appl Crystallogr 32:837

Figure Captions

Fig. 1 Isothermal section of the La–B–C phase diagram at 1270 K. Dashed tie-lines correspond to equilibria in the solid state below 1190 K and $La_{15}B_{14}C_{19}$ observed in arc-cast samples.

Fig. 2 Secondary electron image (a) and x-ray powder pattern (b) of the annealed bulk sample with nominal atomic composition La/B/C = 14/32/54. Indicated (*) reflections are from LaB_6 and other of ~$La_7B_9C_{34}$. Backscattered electron image (c) and x-ray powder pattern (d) of the annealed bulk sample with nominal atomic composition La/B/C = 40/45/15. Indicated (*) reflections are from LaB_4, (•) LaBC and (+) La.

Fig. 3 Crystal structure of ~$La_5B_2C_6$ (a). The chains of edge-sharing La_6C octahedra are emphasized. The rare earth metal atoms environments of discrete carbon atoms (b) and C-B/C-B/C-C (c) units are shown. Lanthanum atoms in (b) and (c) are represented by their anisotropic displacement ellipsoids at the 99.9% probability level.

Fig. 4 Comparison of observed and calculated neutron powder profiles for $La_5B_2C_{4.6}$

Table 1 Crystallographic data of ternary compounds in the La–B–C system

Compound	Space group	Structure type	Unit cell parameters (Å)			References
			a	*b*	*c*	
$La_5(BC)_x$ ($5.6 \le x \le 8.8$)	*P*4/*ncc*	$La_5B_2C_6$	8.584(1)-8.598(1)		12.315(2) - 12.730(1)	[10], [a]
$La_5B_4C_{5-x}$ ($x=0.15$)	*Pna*2$_1$	$Ce_5B_4C_5$	24.682(3)	8.612(1)	8.647(1 b)	[15], [a]
LaBC	*P*2$_1$2$_1$2$_1$	LaBC	8.666(1)	8.707(1)	12.485(2)	[13], [a]
$La_{10}B_9C_{12}$	*P*4$_1$2$_1$2	$Ce_{10}B_9C_{12}$	8.6678(5)		25.689(3)	[14], [a]
$La_{15}B_{14}C_{19}$ [b]	*P*2$_1$/c	$La_{15}B_{14}C_{19}$	8.640(3)	8.636(4) β=94.28(3)°	19.823(6)	[16], [a]
LaB_2C_2	*P*4/*mbm*	LaB_2C_2	5.4050(2)		3.9623(2)	[8], [a]
~$La_4B_3C_{12}$	---	---	---	---	---	
~$La_4B_5C_{18}$	---	---	---	---	---	

[a] Powder data of the present work, [b] observed in arc-cast samples.

Table 2 Crystallographic and chemical composition data for alloys $La_5(BC)_x$ ($5.6 \le x \le 8.8$)

Composition	Lattice parameters (*a*, *c* in Å)	*c*/*a*	*V*(Å^3)	B, at %[1)]	(C1-C2/B2) occupation	C3 occupation
$La_5B_{2.8}C_6$	8.622(1) 12.843(4)	1.489	955.0(4)	21(1)	1.00	1.00
$La_5B_{2.8}C_{5.7}$	8.5837(1) 12.7632(2)	1.487	940.39(4)	20(1)	1.00	0.75(4)
$La_5B_{2.4}C_{5.3}$ [2)]	8.5807(1) 12.6539(3)	1.474	931.70(4)	19(1)	0.8(1)	0.50(4)
$La_5B_2C_{4.6}$ [3)]	8.5810(1) 12.5140(2)	1.458	921.44(4)	17(1)	0.8(1)	0.20(3)
$La_5B_{1.8}C_{3.9}$	8.5746(4) 12.437(1)	1.450	914.4(2)	16(1)	0.7(2)	0.10(5)
$La_5B_{1.75}C_{3.8}$ [4)]	8.578(1) 12.342(2)	1.438	908.3(3)	16(1)	0.7(2)	0.0
$La_5B_{1.5}C_{4.1}$	8.584(1) 12.315(2)	1.434	907.5(4)	15(1)	0.7(2)	0.0

[1)] WDX microprobe analyses
[2)] Chemical analysis in at % :La-38.1, B-19.0, C-42.9
[3)] Neutron powder diffraction data
[4)] Synchrotron single crystal diffraction data

Table 3 Comparison of refinement results by synchrotron single crystal and neutron powder diffraction data of ~$La_5B_2C_6$ [a)]

Methode		Neutron powder data [b)]	Synchrothron single-crystal data [c)]
Composition		$La_5B_2C_{4.6}$	$La_5B_{1.75}C_{3.8}$
La1	*x*	0.6502(3)	0.64998(3)
	y	0.0508(3)	0.05149(2)
	z	0.1083(3)	0.10687(2)
	B_{eq}	0.38(2)	0.86(1)
La2	*z*	0.1363(6)	0.13729(4)
	B_{eq}	0.76(3)	1.10(1)
C1	*x*	0.6545(5)	0.6550(6)
	y	0.0457(6)	0.0448(6)
	z	-0.09351(4)	-0.0890(4)
	B_{iso}	0.98(3)	1.03(1)
C2/B2	*x*	0.6269(5)	0.6292(6)
	y	0.0632(6)	0.0609(6)
	z	-0.2010(3)	-0.2000(4)
	B_{iso}	1.16(3)	1.46(1)
C3	*z*	0.357(1)	
	B_{iso}	1.51(3)	
Occupancy:			
	C1	0.80(1)	0.7(2)
	C2/B2	0.30(1)/0.50(1)	0.3(2)/0.4(2)
	C3	0.20(3)	-

[a)] La2 and C3 in 4c (1/4, 1/4, *z*)
[b)] R_I=0.067, R_F=0.056, R_p=0.10 , R_{exp}=0.14, χ^2=1.7
[c)] *R*1=0.035, *wR*2=0.087 for 2997 reflections with $I<2\sigma(I_o)$.

Table 4
Anisotropic displacement parameters for lanthanum atoms in ~$La_5B_2C_6$

Atom	B_{11}	B_{22}	B_{33}	B_{23}	B_{13}	B_{12}
La1 [a)]	0.32(2)	0.40(3)	1.25(6)	0.002(6)	-0.0022(9)	-0.010(7)
La2 [a)]	0.30(2)	B_{22}	1.88(1)	0.000	0.000	0.000
La1 [b)]	0.501(6)	0.656(7)	1.68(1)	0.004(4)	-0.0059(6)	-0.021(5)
La2 [b)]	0.466(9)	B_{22}	2.28(1)	0.000	0.000	0.000

[a)] neutron powder diffraction data
[b)] synchrotron single crystal data

Fig. 1 Isothermal section of the La–B–C phase diagram at 1270 K. Dashed tie-lines correspond to equilibria in the solid state below 1190 K and $La_{15}B_{14}C_{19}$ observed in arc-cast samples.

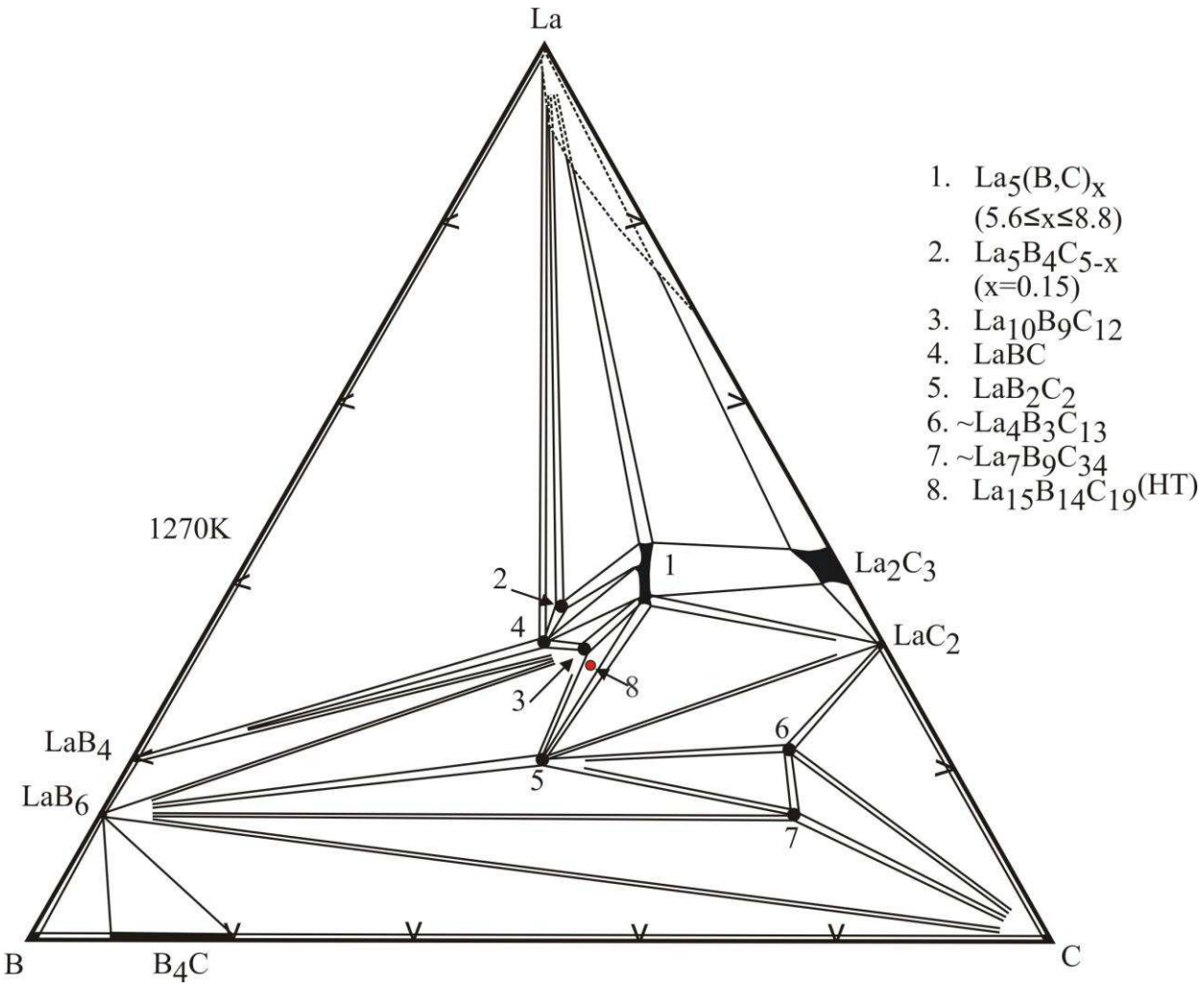

Fig. 2 Secondary electron image (a) and x-ray powder pattern (b) of the annealed bulk sample with nominal atomic composition La/B/C = 14/32/54. Indicated (*) reflections are from LaB_6 and other reflections are of ~$La_7B_9C_{34}$. Backscattered electron image (c) and x-ray powder pattern (d) of the annealed bulk sample with nominal atomic composition La/B/C = 40/45/15. Indicated (*) reflections are from LaB_4, (•) LaBC and (+) La.

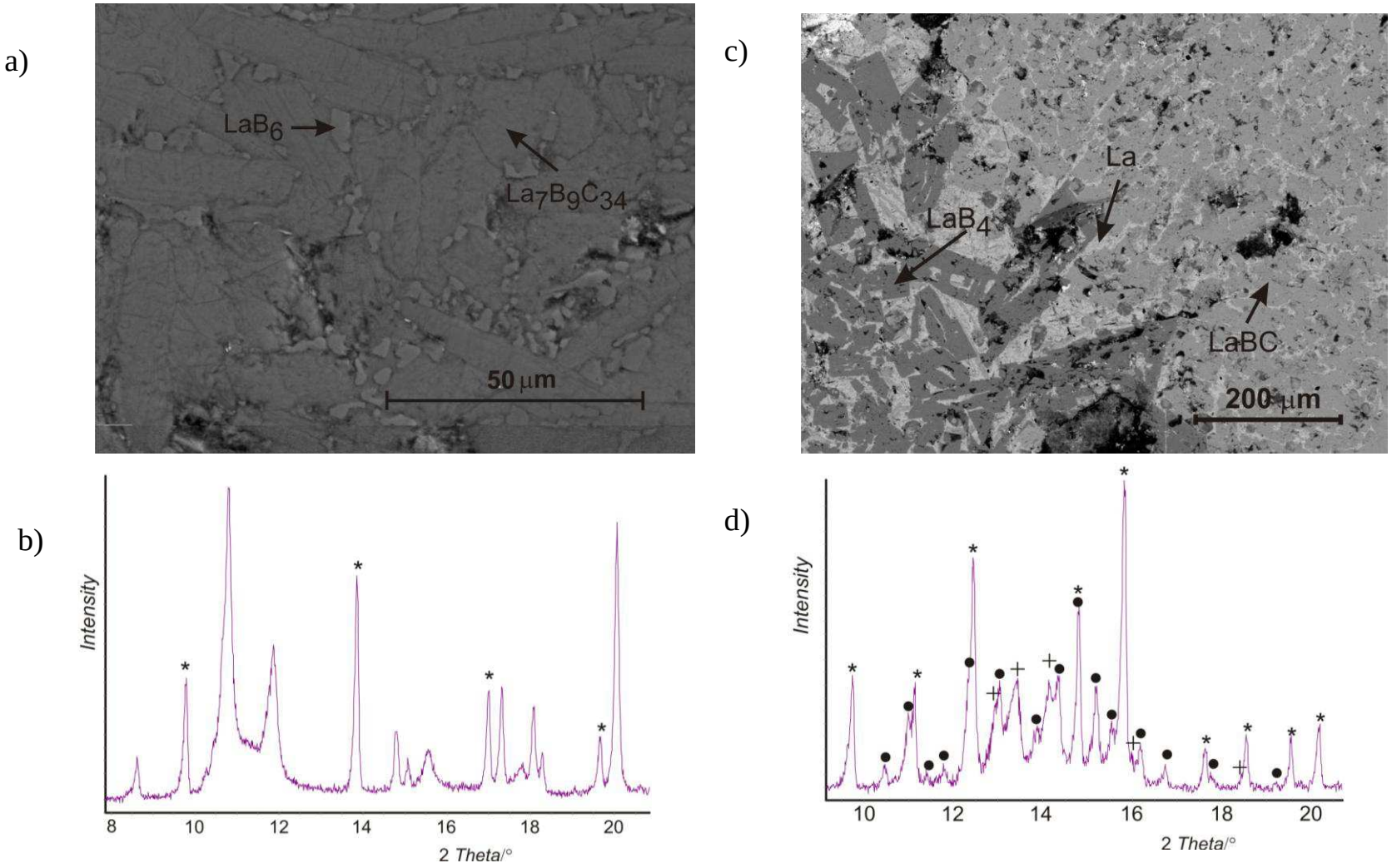

Fig. 3 Crystal structure of ~$La_5B_2C_6$ (a). The chains of edge-sharing La_6C octahedra are emphasized. The rare earth metal atoms environments of discrete carbon atoms (b) and C-B/C-B/C-C (c) units are shown. Lanthanum atoms in (b) and (c) are represented by their anisotropic displacement ellipsoids at the 99.9% probability level.

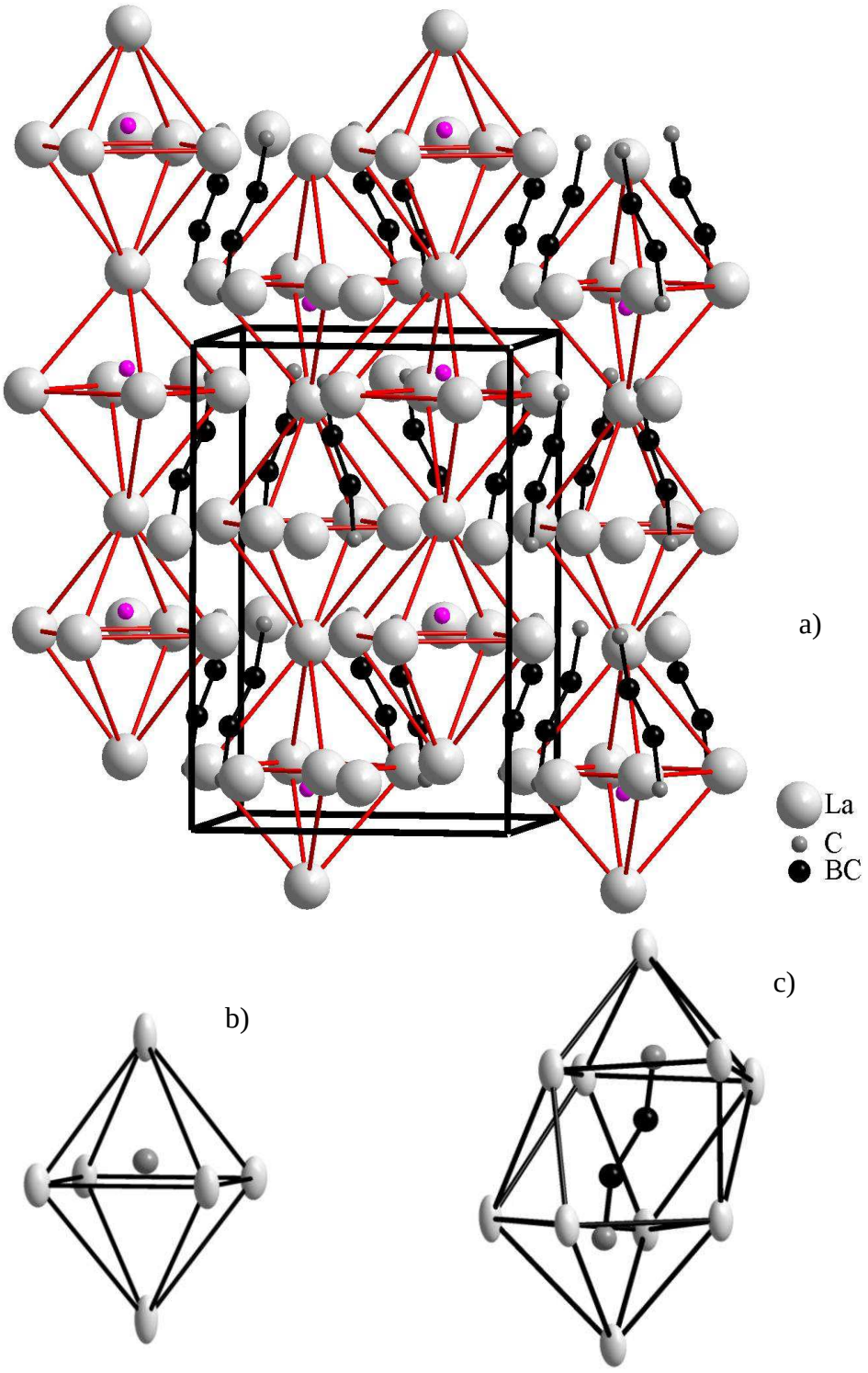

Fig. 4. Comparison of observed and calculated neutron powder profiles for $La_5B_2C_{4.6}$

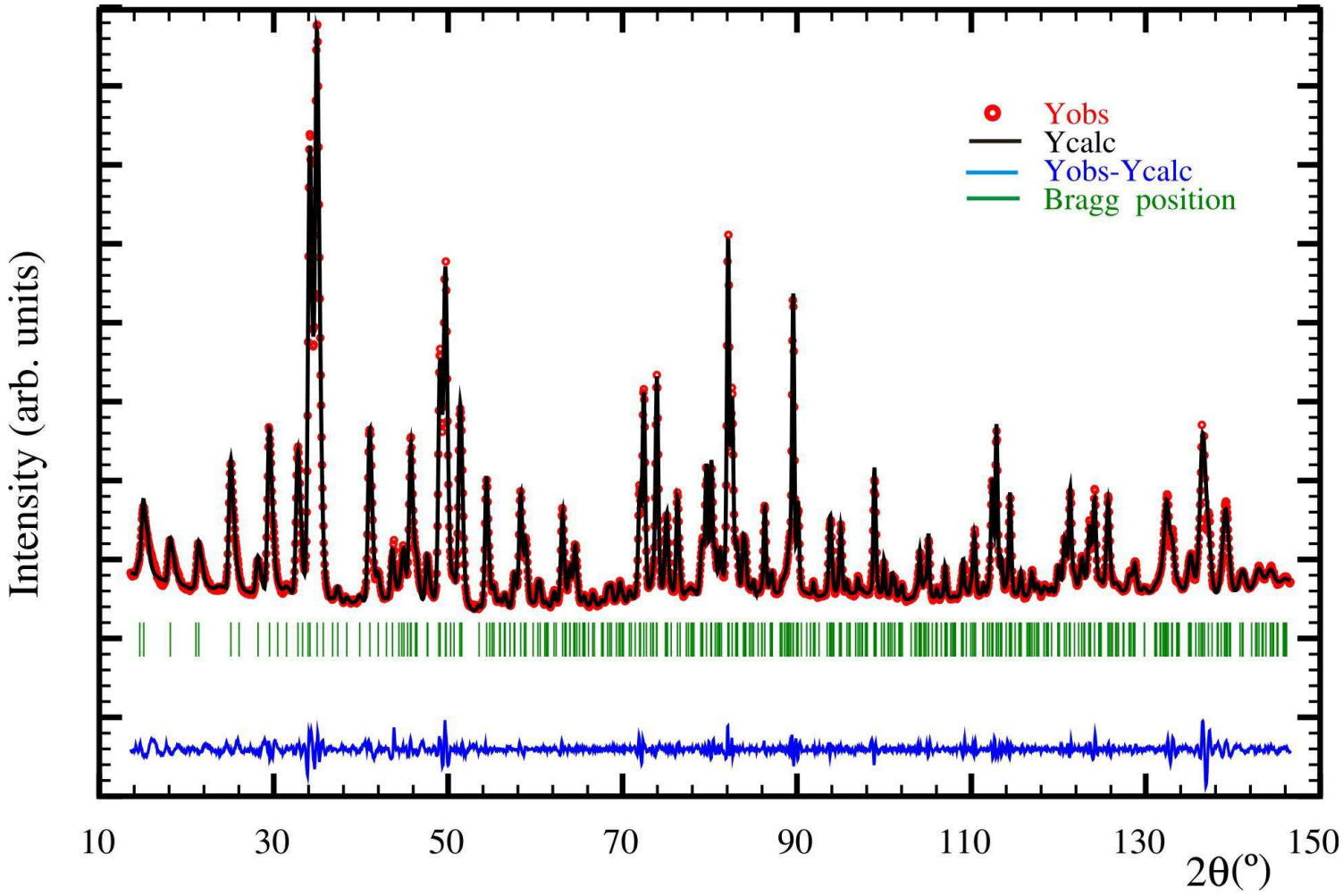

Graphics for use in the Table of Contents